Characterization of $LaCrO_4$ and $NdCrO_4$ by XRD, Raman Spectroscopy, and ab Initio Molecular Orbital Calculations

Yoshitaka Aoki, Hidetaka Konno,* Hiroto Tachikawa, and Michio Inagaki†

Graduate School of Engineering, Hokkaido University, Kita-ku, Sapporo 060-8628

†Aichi Institute of Technology, Yakusa, Toyota 470-0392

(Received December 13, 1999)

Single phase $LnCrO_4$ (Ln = La–Nd) compounds were attempted to synthesize by the pyrolysis of precursors prepared from Ln^{III}–Cr^{VI} mixed solutions. Only $LaCrO_4$ and $NdCrO_4$ were obtained as a single phase. $LaCrO_4$ was monazite type (monoclinic, $P2_1/n$), as reported, and the cell parameters were refined to be a = 0.70369, b = 0.72348, c = 0.66918 nm and β = 104.950° by an X-ray Rietveld method. $NdCrO_4$ was zircon type (tetragonal, $I4_1/amd$) and the cell parameters were a = 0.73107 and c = 0.66999 nm. It was found that CrO_4^{3-} tetrahedra in $LaCrO_4$ have C_1 symmetry and the four Cr–O bond lengths are different, whereas those in $NdCrO_4$ have D_{2d} symmetry and all Cr–O bond lengths are 0.1702 nm. Detailed Raman spectra of $LaCrO_4$ and $NdCrO_4$ were measured and assigned to the vibrational modes of the CrO_4^{3-} tetrahedra. Molecular orbital calculations indicated that the charge density on the chromium ions in the tetrahedra is much less than the nominal 5+ due to the migratory electrons from oxygen atoms, and nearly the same irrespective of the symmetry of tetrahedron, suggesting that the Cr–O bonds are strongly covalent in nature.

Compounds containing the unusual valence state of Cr^V have been studied mainly because of their magnetic properties.[1—4] Recently, Li_3CrO_4 was reported to show hopping conduction of d^1 electrons on Cr^V [5] and Li^+ ion conductivity.[6] Li_3CrO_4, however, is not stable in the ambient atmosphere, whereas Cr^V compounds of rare earth elements (Ln), $LnCrO_4$, are stable in air, even at considerably high temperatures. $LnCrO_4$ compounds have been synthesized by (a) the reaction of $Ln_2(CrO_4)_3$ with Ln_2O_3 or $Ln(NO_3)_3 \cdot nH_2O$ at elevated temperatures,[7—9] (b) the thermal decomposition of $LnCr(C_2O_4)_3 \cdot nH_2O$ (Ln = La, Pr, Nd, and n depends on Ln) in air[10,11] or (c) the reaction of $Cr(NO_3)_3 \cdot 9H_2O$ with $Ln(NO_3)_3 \cdot 6H_2O$ (Ln = Nd, Sm, and Eu) at elevated temperatures.[7—9,12] $LaCrO_4$ has a monoclinic structure similar to that of monazite,[7,13] and $LnCrO_4$ compounds containing rare earth elements having a larger atomic number than Nd are reported to have a tetragonal structure similar to that of zircon.[2,12] It was also reported that by using method (a) the synthesis of $CeCrO_4$ was unsuccessful[11] and $PrCrO_4$ was always obtained as a mixture of monoclinic and tetragonal structures.[8] It, however, was claimed that monoclinic single phase $PrCrO_4$ was formed by method (b) and characterized by IR spectroscopic measurements.[10]

We have reported that $LaCrO_4$ can be synthesized as a single phase by pyrolysis of the precursor prepared from equimolar mixed solutions of La^{III} and Cr^{VI} [13,14] also, the compound was characterized by X-ray photoelectron spectroscopy, XPS, and ab initio molecular orbital calculations.[14] However, the detailed crystal structures, that is, the atomic positions of La, Cr, and O, were not known at that time, so that a simplified model was used for the calculations. In the present work, a series of $LnCrO_4$ (Ln = La, Ce, Pr, and Nd) compounds were attempted to synthesize by our method, if each compound could be obtained as a single phase. For those obtained as a single phase, the atomic positions were determined by Rietveld refinement of powder X-ray diffraction, XRD, data and vibrational structures, which should be affected by the symmetry of CrO_4 tetrahedra were characterized by Raman spectroscopy. Although all vibrational modes of the CrO_4 tetrahedra are Raman active independent of the symmetry, no data have been reported concerning the above mentioned compounds except for monoclinic $PrCrO_4$ by IR spectroscopy.[10] Further, based on the crystalline structure, the electronic state of Cr^V in the compounds was examined by two types of ab initio molecular orbital calculations.

Experimental

$LaCrO_4$ was synthesized by pyrolysis of the precursor at 600 °C for 1 h in air.[13,14] The precursor was prepared by vacuum drying of an equimolar solution of $La(CH_3COO)_3$ and CrO_3 at 70 °C, followed by preheating at 400 °C in air. The details were reported elsewhere.[13] The precursors containing other rare earth elements were prepared by the same procedure with an equimolar solution of $Ln(CH_3COO)_3$ and CrO_3. The pyrolysis conditions of the precursor to form single phase $LnCrO_4$ were investigated by TG-DTA, XRD, and XPS. The details concerning the XPS measurements have been described elsewhere.[14]

The chemical composition of $LnCrO_4$, prepared as a single phase, was determined by chemical analyses with three different samples. About 0.13 g of a $LnCrO_4$ sample was dissolved in 100 cm^3 of a 0.2 mol dm^{-3} H_2SO_4 solution. The $LnCrO_4$ dissolves into a sulfuric acid solution accompanying a disproportionation reaction of Cr^V ions, as follows:

$$3LnCrO_4 + 8H^+ \rightarrow 3Ln^{3+} + 2CrO_4^{2-} + Cr^{3+} + 4H_2O \quad (1)$$

The Ln^{3+} ions were determined by chelate titration with an EDTA solution, and CrO_4^{2-} anions and total chromium ions by redox titration with an Fe^{II} solution. The density of the compounds was measured in CCl_4 using a liquid pycnometer.

X-Ray diffraction patterns were measured by a JEOL 3500 diffractmeter with a monochromator under the following conditions: Cu $K\alpha$, 30 kV, 300 mA; scanning step, 0.02 deg (2θ); counting time, 7—12 s/step. Structure refinement by the Rietveld method was carried out using the RIETAN program.[15] The peak shape was represented by a pseudo-Voigt function.[16] Because the atomic scattering factor and an anomalous dispersion correction for Cr^V were not found, these were assumed to be the same as those of the Cr atom.[16]

Raman spectroscopic measurements were carried out by a triple type monochromator (JASCO NRS-2000) under the irradiation of an argon ion laser (514.2 nm) of 50 mW. During the measurements, a sample, pressed in a disc shape of ca. 10 mm in diameter and 1 mm in thickness, was set on a stainless steel holder and rotated at 600 rpm to avoid decomposition by the laser beam.

Molecular orbital calculations were carried out for CrO_4^{3-} clusters by ab initio restricted open shell Hartree–Fock[17,18] and MP2[17] methods to estimate the net charge on each atom in the clusters. The employed basis sets were Huzinaga's (333/33/3) for the chromium atoms[19] and 6-311+G* for the oxygen atoms.[17] All calculations were performed using the GAUSSIAN 94 program.[17]

Results and Discussion

A. Synthesis of $LnCrO_4$. The thermal decomposition behavior of the Nd-precursor in air showed two plateaus in the region 600—700 °C and above 750 °C in the TG curve, and two endothermic peaks at 570 and 770 °C in the DTA curve. The endothermic peak at 770 °C was due to the formation of perovskite type $NdCrO_3$, which was identified by XRD measurements of the products in the second plateau region. The XRD pattern of the product at 600 °C showed the formation of a zircon type compound, and other impurities were not observed; therefore, the endothermic peak at 570 °C was considered to be due to the formation of $NdCrO_4$. Based on this TG-DTA data, pyrolysis at constant temperatures of around 600 °C was carried out to determine the condition to prepare a $NdCrO_4$ single phase (by XRD); also, pyrolysis at 580 °C for 3 h in air was found to be the most suitable condition. In Fig. 1, the Cr 2p XPS spectrum of $NdCrO_4$ is shown together with that of $LaCrO_4$. Although a slight swelling is observed at the lower binding energy side of the Cr $2p_{3/2}$ peak, the binding energies, E_B, of the Cr $2p_{3/2}$ and Cr $2p_{1/2}$ electrons are 579.0 and 588.3 eV, which is in good agreement with those for $LaCrO_4$.[14] The average chemical composition of $NdCrO_4$ and $LaCrO_4$, prepared as a single phase was $Nd_{0.994}Cr_{1.00}O_{3.99}$ and $La_{0.997}Cr_{1.00}O_{3.99}$, indicating that the deviation from the stoichiometric composition is very small. The Cr^{III}/Cr^{VI} mole ratio resulted by disproportional dissolution was 0.668 for $NdCrO_4$ and 0.666 for $LaCrO_4$, in agreement with Eq. 1; thus, chromium is pentavalent.

The pyrolysis of precursors containing Ce^{III} and Pr^{III} was also carried out to produce $CeCrO_4$ and $PrCrO_4$ by the same method. The Ce-precursor, however, directly decomposed to CeO_2 and Cr_2O_3. This can be attributed to the stability of CeO_2 at elevated temperatures, since it was formed even in an argon atmosphere. The Pr-precursor decomposed to a mixture of monazite type and zircon type compounds and a single phase of $PrCrO_4$ was not obtained under any conditions selected on the basis of TG-DTA data. It was reported that the single phase monazite type $PrCrO_4$ was formed by the decompositions of $Pr[Cr(C_2O_4)_3]$ at 500 °C for 10 min, and transferred to the zircon type by a further heat treatment,[10] though no such phenomena were observed by our method. Our results agreed with other reports[8,11] that no single phase of $PrCrO_4$ has been obtained under normal pressure, because the Pr^{III} ion has a critical ionic radius for a structural change between the monazite and zircon types.

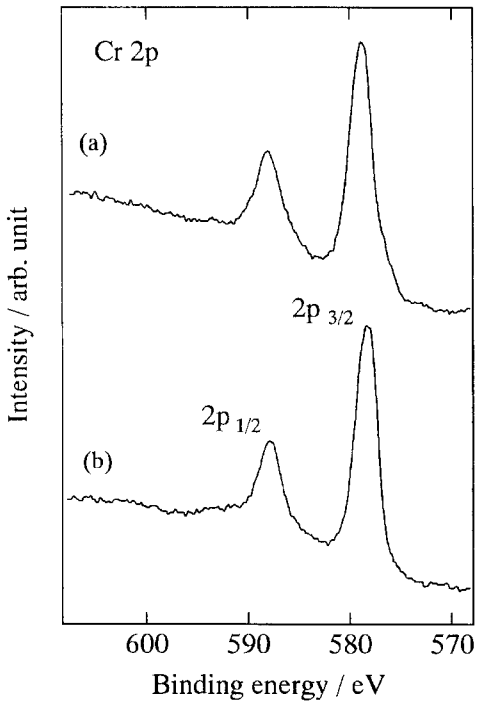

Fig. 1. X-Ray photoelectron spectra of Cr 2p for $NdCrO_4$ (a) and $LaCrO_4$ (b).

B. Structural Analysis. The d-spacing, relative intensity and *hkl* index for $NdCrO_4$ (zircon type, S.G. $I4_1/amd$) and $LaCrO_4$ (monazite type, S.G. $P2_1/n$) are summarized in Table 1, and crystallographic data together with reliability factors of Riedveld refinement are given in Table 2. Although the refinement was carried out up to $2\theta = 110°$ for $NdCrO_4$ and 100° for $LaCrO_4$, the peaks at larger 2θ are omitted in Table 1 due to a space limitation. The observed d-spacing and *hkl* indexing for both compounds are slightly different from those[20,21] cited in the JCPDS index. In addition, additional peaks in diffraction patterns that were not previously recorded were identified by the present study. These peaks lie in the relative intensity range of 1—25%. Although the differences in the calculated lattice constants were less than 1%, they produced a 2% difference in the calculated density of $LaCrO_4$. The measured densities of $NdCrO_4$ and $LaCrO_4$ were 5.053 and 5.148 $g\,cm^{-3}$, respectively, indicating that

Table 1. The Observed and Calculated d-Spacing in nm, Relative Intensity and hkl Indexing of XRD Powder Patterns for $LaCrO_4$ and $NdCrO_4$

hkl	d_{obs} / nm	d_{calc} / nm	I/I_0	hkl	d_{obs}	d_{calc}	I/I_0
	$NdCrO_4$			301	0.1984	0.1985	3
101	0.4811	0.4813	25	$\bar{2}31$	0.1964	0.1965	8
200	0.3653	0.3654	100	$\bar{1}32$	0.1939	0.1940	31
211	0.2909	0.2911	8	320*, 103	0.19203	0.19200	18
112	0.2720	0.2720	69	$\bar{1}23$	0.18961	0.18961	<1
220	0.2584	0.2584	21	023	0.18512	0.18514	6
202	0.2407	0.2407	3	$\bar{3}22$	0.18365	0.18368	19
301	0.2277	0.2277	14	$\bar{3}03$, 040*	0.18085	0.18087	10
103	0.2048	0.2048	8	$\bar{2}32$, $\bar{2}23$*	0.18032	0.18028	4
321	0.1932	0.1933	13	132	0.17880	0.17881	24
312	0.18739	0.18739	59	140	0.17478	0.17479	12
400	0.18279	0.18277	15	$\bar{1}41$	0.17167	0.17162	<1
213	0.17865	0.17866	4	$\bar{4}11$	0.17090	0.17094	1
411	0.17089	0.17088	3	400*, $\bar{4}02$	0.16949	0.16953	12
420	0.16347	0.16347	13	141	0.16715	0.16598	1
303	0.16054	0.16051	2	410	0.16543	0.16546	6
004	0.16003	0.16002	3	$\bar{3}30$*, $\bar{4}12$	0.16516	0.16515	6
402	0.15872	0.15871	<1	$\bar{2}04$*, $\bar{1}14$	0.16311	0.16311	5
332	0.15171	0.15172	16	312	0.16221	0.16224	3
204	0.14658	0.14657	11	004	0.16164	0.16163	5
501, 431*	0.14257	0.14254	4	033	0.16122	0.16069	<1
413	0.13641	0.13636	2	$\bar{3}32$*, 240	0.15969	0.15972	10
224	0.13606	0.13604	10	$\bar{2}14$	0.15923	0.15921	6
521	0.13283	0.1328	1	$\bar{1}42$, 014*	0.15784	0.15805	3
314	0.13161	0.13157	<1	420	0.15396	0.15383	<1
512	0.13085	0.13084	13	$\bar{4}22$	0.15359	0.15351	2
440	0.12927	0.12924	3	$\bar{1}24$	0.15181	0.15182	5
				322	0.15132	0.15123	1
	$LaCrO_4$			241	0.15074	0.15082	1
$\bar{1}01$	0.5434	0.5438	9	$\bar{2}42$	0.15052	0.15059	2
110	0.4952	0.4954	7	223	0.14925	0.14929	3
011	0.4818	0.4821	14	$\bar{2}24$	0.14874	0.14877	<1
$\bar{1}11$	0.4342	0.4347	18	$\bar{3}14$	0.14814	0.14813	2
101	0.4176	0.4178	6	024	0.14751	0.14757	<1
111, 020*	0.3616	0.3617	24	421, $\bar{4}31$*	0.14223	0.14224	4
200	0.3396	0.3399	6	$\bar{4}23$	0.14189	0.14184	2
002	0.3229	0.3226	4	340	0.14139	0.14137	4
120	0.3191	0.3194	100	$\bar{1}43$	0.14037	0.14038	1
021	0.3156	0.3157	1	$\bar{1}51$	0.13982	0.13983	1
210, $\bar{2}11$	0.3075	0.3076	16	$\bar{3}24$	0.13956	0.13961	2
$\bar{1}12$	0.2974	0.2975	25	303	0.13927	0.13926	1
012	0.2949	0.2951	67	043	0.13857	0.13854	1
$\bar{2}02$	0.2718	0.2719	20	124*, $\bar{1}34$	0.13757	0.13757	14
$\bar{2}12$	0.2543	0.2545	21	332	0.13704	0.13700	8
112	0.2500	0.2501	11	402	0.13665	0.13662	2
220, $\bar{2}21$	0.2476	0.2476	7				
$\bar{1}22$	0.2423	0.2423	4				
$\bar{3}01$	0.2334	0.2335	3				
130	0.2274	0.2273	1				
031	0.2259	0.2260	14				
$\bar{1}03$, $\bar{3}11$	0.2223	0.2224	27				
221, $\bar{2}22$	0.2179	0.2180	12				
310	0.2163	0.2163	1				
$\bar{1}13$	0.2127	0.2128	<1				
131	0.2088	0.2089	2				
$\bar{3}12$	0.2044	0.2045	2				
212	0.2006	0.2007	34				

* Greater peaks than the others in that siries.

Table 2. Summary and Reliability Factors of Rietveld Refinement

	$NdCrO_4$	$LaCrO_4$
Space group	$I4_1/amd$	$P2_1/n$
Crystal system	Tetragonal	Monoclinic
Z	4	4
No. of reflection	136	702
Lattice constants	a=0.73107(1) nm	a=0.70369(1) nm
	c=0.63999(1) nm	b=0.72348(1) nm
		c=0.66918(1) nm
		β=104.950(4) deg
$D_X/g\,cm^{-3}$	5.0534	5.1485
R_{wp}	12.39	9.03
R_p	9.45	7.03
R_F	2.29	0.90
R_I	3.19	1.52
G of F	1.11	1.22

our results are more accurate. The results of a Rietveld refinement for $NdCrO_4$ and $LaCrO_4$ are shown in Fig. 2, where the calculated values are plotted by dots; the agreement is so excellent, as shown by the difference curve, that they are not distinguishable. In the refinement of $NdCrO_4$, $NdVO_4$ was used as a starting model for the initial atomic position and thermal parameters,[22] and isotropic thermal parameters B were employed. The starting model of $LaCrO_4$ was $LaVO_4$.[23] As shown in Table 2, the reliability factors (R_{wp}, R_p, R_F, and R_{exp}) are sufficiently small, and G of F factor (goodness of fitting indicator: R_{wp}/R_{exp}), which represents the quality of the refined structure, is less than the required limit of 1.3.

The atomic positions and bond lengths are listed in Tables 3 and 4. Based on these data, bond length/bond strength calculations for Cr were carried out by a method of Brown and Shannon[24] with constants of Brown and Altermatt.[25] These calculations were carried out as a test to assure that the structure model by a Rietveld refinement is consistent with the component species, since the bond strength is equivalent to the valence of metal estimated by the metal-oxygen bond length. The calculated values were 5.07+ for Cr^{5+} ion in

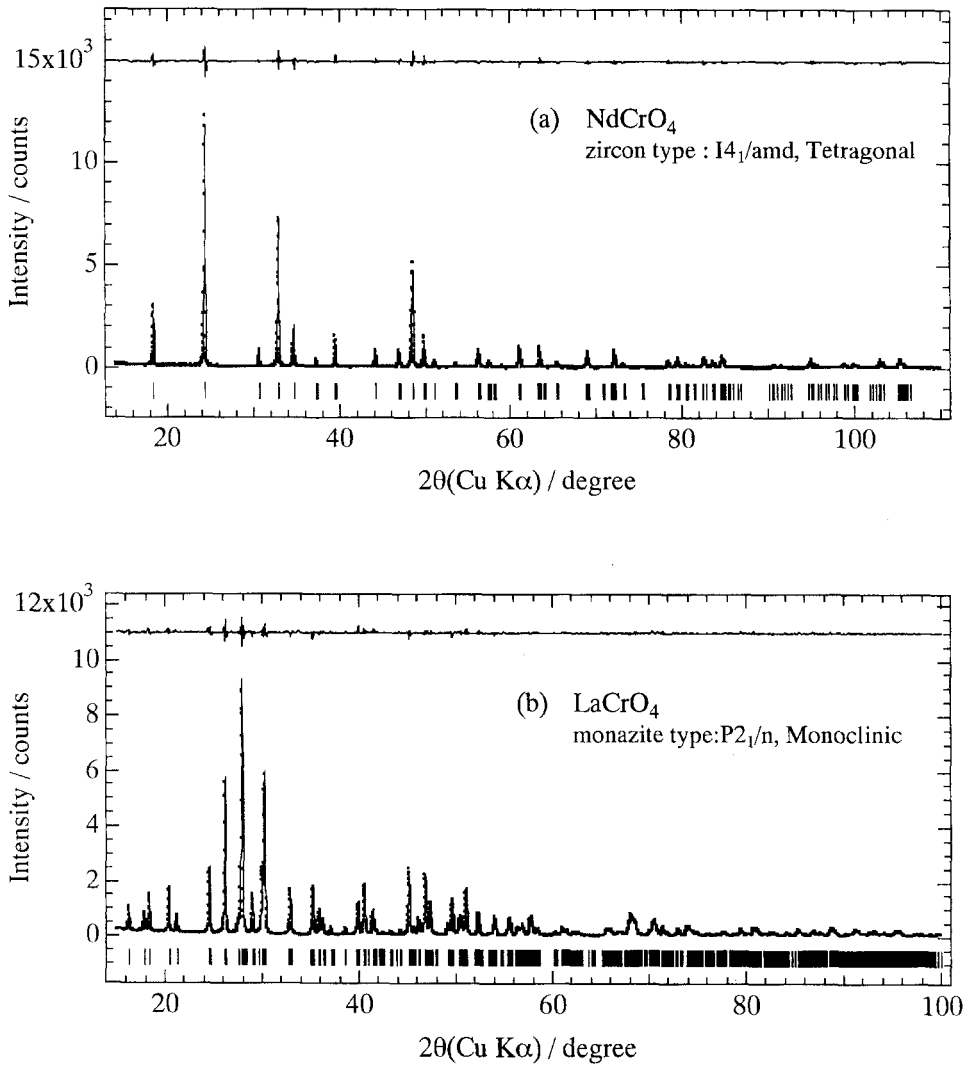

Fig. 2. The powder X-ray diffraction pattern and Rietveld refinement profiles for (a) $NdCrO_4$ and (b) $LaCrO_4$. The full lines and dots show observed and calculated patterns respectively. Tick marks indicate the positions of allowed Bragg reflections. The difference between the observed and calculated values is located at the top.

Table 3. Atomic Positions and Thermal Displacement Parameters in nm^2 for $NdCrO_4$ and $LaCrO_4$

Atom	Site	x	y	z	B
			$NdCrO_4$		
Nd	4a	0.0000	0.7500	0.1250	0.0037
Cr	4b	0.0000	0.2500	0.3750	0.0011
O	16h	0.0000	0.4305(1)	0.2071(1)	0.0089
			$LaCrO_4$		
La	4e	0.2782(1)	0.1568(1)	0.1029(1)	0.0047
Cr	4e	0.3010(1)	0.1657(1)	0.6144(1)	0.0011
O(1)	4e	0.2416(3)	−0.0032(2)	0.4232(3)	0.0139
O(2)	4e	0.3892(3)	0.3394(4)	0.4921(3)	0.0060
O(3)	4e	0.4852(2)	0.1129(1)	0.8239(1)	0.0125
O(4)	4e	0.1206(2)	0.2098(1)	0.7295(2)	0.0099

Table 4. Selected Bond Lengths in nm and Symmetry of CrO_4^{3-} Units in $NdCrO_4$ and $LaCrO_4$

$NdCrO_4$		$LaCrO_4$	
Nd–O	C.N. 8	La–O	C.N. 9
0.2394(1)×4		La–O(1)×2	0.2466(3), 0.2507(4)
0.2501(2)×4		La–O(2)×3	0.2585(5), 0.2645(4), 0.2845(5)
		La–O(3)×2	0.2666(2), 0.2530(2)
		La–O(4)×2	0.2531(3), 0.2481(2)
Cr–O	C.N. 4	Cr–O	C.N. 4
0.1702(1)×4		Cr–O(1)	0.1741(4)
		Cr–O(2)	0.1702(4)
O–O in CrO_4^{3-} units		Cr–O(3)	0.1690(2)
0.2838(4)×4		Cr–O(4)	0.1681(3)
0.2639(4)×2		Average	0.1703
Symmetry of CrO_4^{3-} unit		Symmetry of CrO_4^{3-} unit	
D_{2d}		C_1	

$NdCrO_4$ and 5.08+ in $LaCrO_4$, showing that the structural parameters of $NdCrO_4$ and $LaCrO_4$ are sufficiently accurate.

The structures of $LnCrO_4$ constructed based on the data given in Tables 2 and 3 are shown in Fig. 3. In both compounds, the Ln^{3+} ions have a larger coordination number than does the Cr^{5+} ion. The zircon type structure $NdCrO_4$ is built from chains of alternating edge-sharing CrO_4^{3-} tetrahedra and NdO_8 bisdisphenoids. This CrO_4^{3-} tetrahedron is slightly elongated, and its symmetry is D_{2d}, because the O–O edges shared with NdO_8 are shorter than the length of the unshared tetrahedral edges. The monazite type structure $LaCrO_4$ is more complex; four Cr–O bonds of the CrO_4^{3-} tetrahedron have different lengths, and the symmetry of this tetrahedron is C_1. The La^{3+} ions have a rather uncommon coordination number of nine. These results are in good agreement with the characteristics of other monazite type compounds.[23] Although it is hard to describe the presence of chains of the CrO_4^{3-} tetrahedra and LaO_9 polyhedra, one La^{3+} ion locates very near to one Cr^{5+} ion, having a distance of 0.355 nm. It is worth noting here that the average Cr–O bond length in $LaCrO_4$ is nearly equal to that of Cr–O in $NdCrO_4$.

C. Vibrational Spectrum Analysis. The IR spectra of CrO_4^{3-} tetrahedra are reported for monazite type $PrCrO_4$ [10] and whitelockite type $Ae_3(CrO_4)_2$ (Ae = Ca, Sr or Ba),[26] though IR measurements provide only the ν_3 (antisymmetric-stretching) and ν_4 (antisymmetric-bending) modes, and the ν_1 (symmetric-stretching) and ν_2 (symmetric-bending) modes are either absent or very weak. Accordingly, no comprehensive vibrational spectra of CrO_4^{3-} tetrahedra have been reported so far. All four tetrahedral modes are active to Raman scattering, which allows us to obtain wider insight into the vibrational structures of $NdCrO_4$ and $LaCrO_4$.

The Raman spectra of both compounds are shown in Fig. 4. Both spectra are composed of strong peaks around 830 cm^{-1} and very weak peaks in the range 200—450 cm^{-1}. Since the bond length of Cr–O is much shorter compared to that of

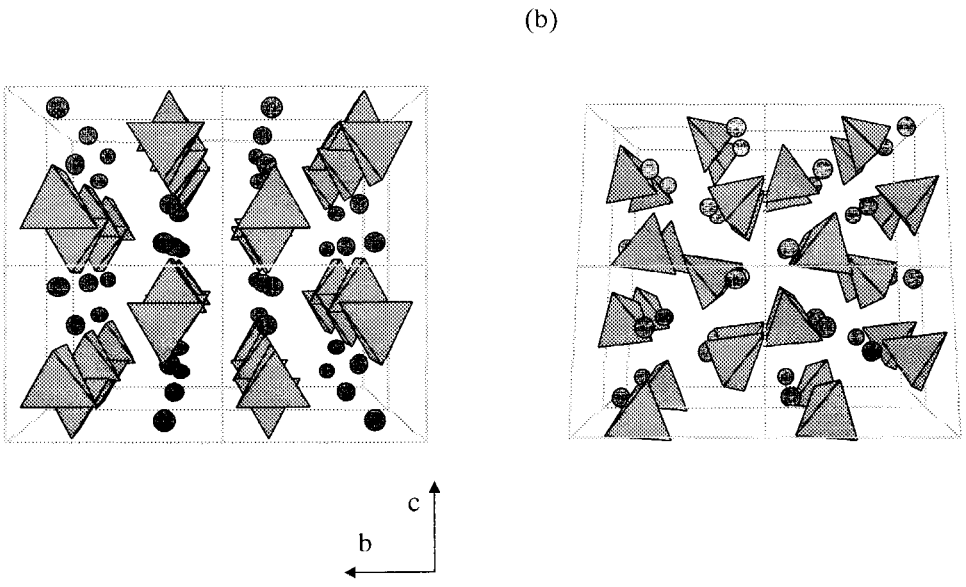

Fig. 3. The perspective projections along a-direction of 2×2×2 units of (a) $NdCrO_4$ and (b) $LaCrO_4$. Ln^{3+} ions are shown as dark spheres and CrO_4^{3-} units are represented by gray tetrahedra.

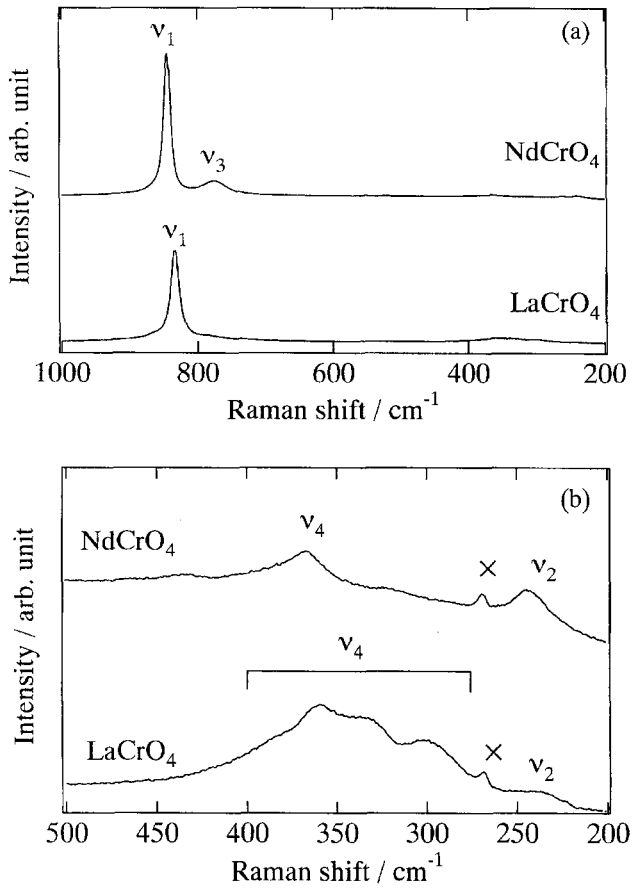

Fig. 4. Raman spectra for $NdCrO_4$ and $LaCrO_4$ of (a) strong stretching modes and (b) weak bending modes. ×: carbon dioxide.

Ln–O, the spectra are attributed to vibration of the CrO_4^{3-} tetrahedron; and are assigned as shown in Fig. 4. It is based on the data of zircon type $CaCrO_4$ [26] containing the $Cr^{VI}O_4^{2-}$ tetrahedron; also, the general rule is that in tetraoxometallate, the ν_1 and ν_3 modes appear in a larger wave number region than ν_2 and ν_4 modes, and the intensity of the ν_1 peaks is strongest and the ν_2 peaks weakest.[27] For $NdCrO_4$, the ν_1 peak appears at a larger wave number than that of ν_3, in contrast to the observation that, for most of tetraoxometallate, the ν_1 appears at a smaller wave number than ν_3.[27] The ν_2 peak is weak, but clearly observed. The spectral assignment for the distorted CrO_4^{3-} tetrahedron of $LaCrO_4$ is more complicated. First, the ν_3 peak is indistinguishable and the ν_1 peak is broader than that of $NdCrO_4$. Second, the region of the ν_2 and ν_4 peaks is composed of several broad peaks. These features suggest that the degeneration of the vibrational modes splits due to a distortion of the tetrahedra. The triply degenerated ν_3 and ν_4 modes can split into three peaks, and the doubly degenerated ν_2 mode can split into two peaks. The disappearance of the ν_3 peak seems to be the result of splitting, by which the peaks are broadened and absorbed into the strong ν_1 peak. The spectral change in the region 200—450 cm^{-1} can also be explained by this splitting. The ν_4 mode region obviously splits into three peaks at 303.5, 334.3, and 384.8 cm^{-1}, which are smaller in wave number than the IR peaks of isomorphic $PrCrO_4$.[10] The ν_4 mode region is also broad and weak, showing the feature of degeneration. There may be a possibility to separate the peaks which originate from the ν_2 mode, but so far it is not appropriate to carry out this without a more accurate theoretical basis. The apparent peak positions are summarized in Table 5. These features of the Raman spectra for $NdCrO_4$ and $LaCrO_4$ support the structure models built from a Rietveld refinement.

D. ab Initio Molecular Orbital Calculation. Using the obtained Cr–O bond lengths and angles, molecular orbital calculations were carried out without any assumption concerning the structure of the CrO_4^{3-} tetrahedra to estimate the charge densities on chromium and oxygen atoms in $NdCrO_4$ and $LaCrO_4$. Because the ionic character of these compounds may be as strong as La_2O_3, $LaPO_4$ or $LaVO_4$,[14,27] calculations were carried out on an isolated CrO_4^{3-} cluster model having different symmetry.

The results obtained by Hartree–Fock and MP2 methods are listed in Table 6. Although the Hartree–Fock method tends to give a more positive charge density on the chromium atoms and a more negative one on the oxygen atoms than those by the MP2 method, the difference between the D_{2d} symmetric and the C_1 distorted CrO_4^{3-} clusters is negligible. In a previous paper,[14] we calculated the values by an ab initio ROHF-MO method assuming a symmetric T_d cluster model having a Cr–O bond length of 0.16 nm for $LaCrO_4$, since information on the atomic position was not available at that time. The previous values were 2.4+ on the Cr atom and 1.3– on the oxygen atoms and not so different from the present results.

These results indicate that the charge distribution in both types of tetrahedron are nearly the same, and that electrons flow into chromium atom from oxygen atoms; that is, the charge density on the chromium atom is much less than the nominal 5+. This implies that the charge distribution in these tetrahedra is insensitive to the symmetry, and the Cr–O bonds are strongly covalent in nature. This covalency may

Table 5. Wavenumber in cm^{-1} of the Raman Spectra for CrO_4^{3-} Tetrahedron in $NdCrO_4$ and $LaCrO_4$

Stretching mode	$NdCrO_4$	$LaCrO_4$
ν_1	844.0	830.0
ν_2	240.3	231.5, 239.1
ν_3	775.8	
ν_4	363.9	303.5, 334.3, 384.8

Table 6. Calculated Charges on Atoms in CrO_4^{3-} Clusters by Hartree–Fock and MP2 Methods

	D_{2d}			C_1	
	Hartree–Fock	MP2		Hartree–Fock	MP2
Cr	2.69+	2.27+	Cr	2.66+	2.26+
O	1.42–	1.32–	O(1)	1.42–	1.34–
			O(2)	1.47–	1.35–
			O(3)	1.33–	1.23–
			O(4)	1.45–	1.33–

make the unusual valence state of chromium(V) stable in the CrO_4^{3-} tetrahedra of both compounds.

Conclusions

Single phase $LaCrO_4$ (monazite type) and $NdCrO_4$ (zircon type) were synthesized by the pyrolysis of precursors prepared from La^{III}–Cr^{VI} and Nd^{III}–Cr^{VI} mixed solutions. The atomic positions in both compounds were determined from XRD data by a Rietveld refinement with good fitting. Based on the crystallographic data, the Raman spectra for the C_1 symmetric CrO_4^{3-} tetrahedra in $LaCrO_4$ and the D_{2d} symmetric ones in $NdCrO_4$ were measured, and four vibrational modes were assigned. It was observed that degeneration due to C_1 symmetry caused a splitting of the ν_2 mode as well as the ν_4 mode. Molecular orbital calculations indicated that the charge density on the chromium ion in the tetrahedra is much less than the nominal 5+ due to migratory electrons from oxygen atoms and nearly the same, irrespective of T_d, D_{2d}, and C_1 symmetry of CrO_4^{3-} tetrahedron, suggesting that the Cr–O bonds are strongly covalent in nature. It is concluded that this charge distribution is a reason for the stability of the unusual valence state of Cr^V.

References

1 A. Morales-Sanchez, F. Fernandez, and R. Saez-Puche, *J. Alloy. Comp.*, **201**, 161 (1993).

2 H. Walter, H. G. Kahle, K. Mulder, H. C. Schopper, and H. Schwarz, *Int. J. Magn.*, **5**, 129 (1973).

3 M. Steiner, H. Dachs, and H. Ott, *Solid State Commun.*, **29**, 231 (1979).

4 G. Buisson, F. Tcheou, F. Sayetat, and K. Scheuemann, *Solid State Commun.*, **18**, 871 (1976).

5 M. A. K. L. Dissanayake, S. Garcia-Martin, R. Saez-Puche, H. H. Sumathipala, and A. R. West, *J. Mater. Chem.*, **4**, 1307 (1994).

6 S. Garcia-Martin, A. D. Robert, M. A. K. L. Dissanayake, and A. R. West, *Solid State Ionics*, **76**, 309 (1994)

7 H. Schwarz, *Z. Anorg. Allge. Chem.*, **322**, 1 (1963).

8 H. Schwarz, *Z. Anorg. Allge. Chem.*, **322**, 15 (1963).

9 H. Schwarz, *Z. Anorg. Allge. Chem.*, **322**, 129 (1963).

10 S. G. Manca and E. J. Baran, *J. Phys. Chem. Solid.*, **42**, 923 (1981).

11 A. Roy and K. Nag, *J. Inorg. Nucl. Chem.*, **40**, 1501 (1978).

12 H. Schwarz, *Z. Anorg. Allge. Chem.*, **323**, 275 (1963).

13 A. Furusaki, H. Konno, and R. Furuichi, *Nippon Kagaku Kaishi*, **1992**, 612.

14 H. Konno, H. Tachikawa, A. Furusaki, and R. Furuichi, *Anal. Sci.*, **8**, 641 (1992).

15 F. Izumi, H. Asano, H. Murata, and N. Watanabe, *J. Appl. Crystallogr.*, **20**, 411 (1987).

16 "The Rietveld Method," ed by R. A. Young, IUCr/OUP, Oxford (1993).

17 M. J. Frisch, G. W. Trucks, H. B. Schlegel, P. M. W. Gill, B. G. Johnson, M. A. Robb, J. R. Cheeseman, T. Keith, G. A. Petersson, J. A. Montgomery, K. Raghavachari, M. A. Al-Laham, V. G. Zakrzewski, J. V. Ortiz, J. B. Foresman, C. Y. Peng, P. Y. Ayala, W. Chen, M. W. Wong, J. L. Andres, E. S. Replogle, R. Gomperts, R. L. Martin, D. J. Fox, S. Binkley, D. J. Defrees, J. Baker, J. P. Stewart, M. Head-Gordon, C. Gonzalez, and J. A. Pople, "GAUSSIAN 94, Revision B.2," Gaussian Inc., Pittsburgh, PA (1995).

18 C. C. Roothan, *Rev. Mod. Phys.*, **32**, 179 (1960).

19 "Physical Science Data," ed by S. Huzinaga, Elsevier, Amsterdam (1984), Vol. 16.

20 JCPDS 16-880

21 JCPDS 36-93

22 B. C. Chakoumakos, M. M. Abraham, and L. A. Boatner, *J. Solid State Chem.*, **109**, 197 (1994).

23 C. E. Rice and W. R. Robinson, *Acta Crystallogr., Sect. B*, **B32**, 2232 (1976).

24 I. D. Brown and R. D. Shanon, *Acta Crystallogr., Sect. A*, **A29**, 266 (1973).

25 I. D. Brown and D. Altermatt, *Acta Crystallogr., Sect. B*, **B41**, 244 (1985).

26 K. Nakamoto, "Infrared Spectra of Inorganic and Coordination Compounds," USA (1963).

27 A. Muller, E. J. Baran, and R. O. Carer, *Struct. Bonding*, **26**, 81 (1976).

28 K. C. Mishra, I. Osterloh, H. Anton, B. Hannebauer, P. C. Schmidt, and K. H. Johnson, *J. Mater. Res.*, **12**, 2183 (1997).